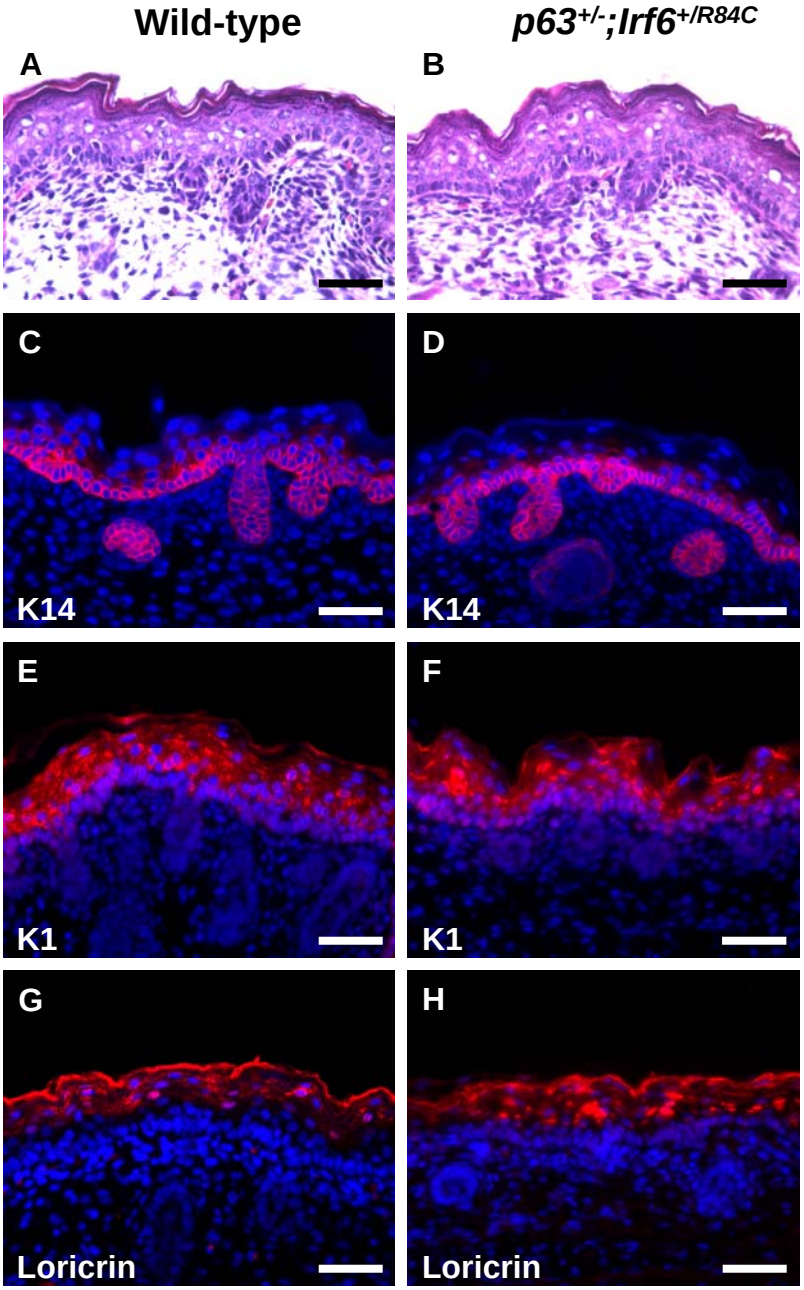

Supplementary Figure 1. Analysis of E18 wild-type and *p63*$^{+/-}$;*Irf6*$^{+/R84C}$ epidermis. (A and B) Histological analyses indicate that the epidermis of *p63*$^{+/-}$;*Irf6*$^{+/R84C}$ mice is indistinguishable from that of their wild-type littermates. (C to H) Immunofluorescence assays confirm that the epidermis of wild-type and *p63*$^{+/-}$;*Irf6*$^{+/R84C}$ mice undergoes an identical differentiation program as judged by expression of keratin 14, keratin 1 and loricrin. Scale bars: 50 µm.

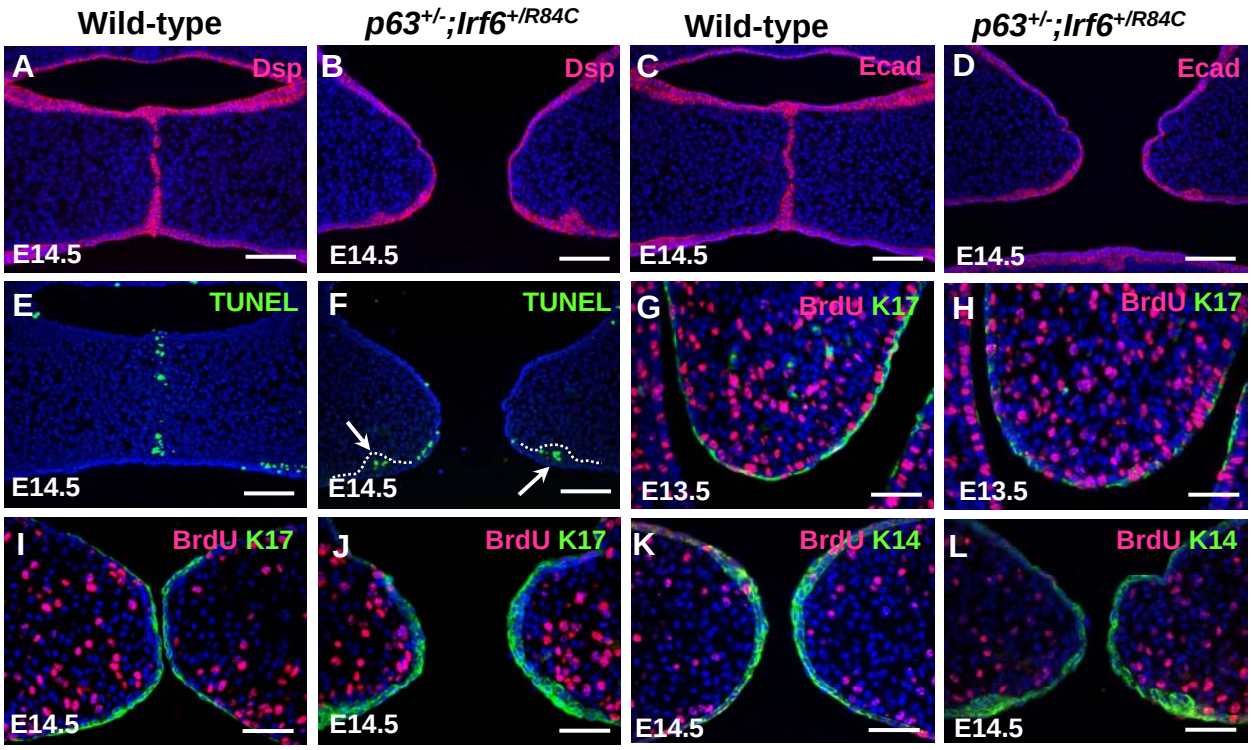

Supplementary Figure 2. Analysis of the MEE of the palatal shelves of wild-type and *p63*$^{+/-}$;*Irf6*$^{+/R84C}$ embryos. (A to D) Immunofluorescence analyses of E14.5 mice indicate that the expression patterns of desmoplakin (A and B) and E-cadherin (C and D) are the same in wild-type and *p63*$^{+/-}$;*Irf6*$^{+/R84C}$ embryos. (E and F) TUNEL assays indicate that cell death was present in the seam and epithelial triangles of wild-type embryos; in contrast, as the palates have not fused in the *p63*$^{+/-}$;*Irf6*$^{+/R84C}$ embryos, cell death was only detected in small islands on the oral surface of the palate (arrowed in F). (G to L) BrdU analyses, in conjunction with keratin 17 (G to J) and keratin 14 (K and L) immunostaining, indicate that neither the abnormal periderm cells nor the basal cells are hyper-proliferative in *p63*$^{+/-}$;*Irf6*$^{+/R84C}$ embryos. Scale bars: A to F, 100 μm; G to L, 50 μm.

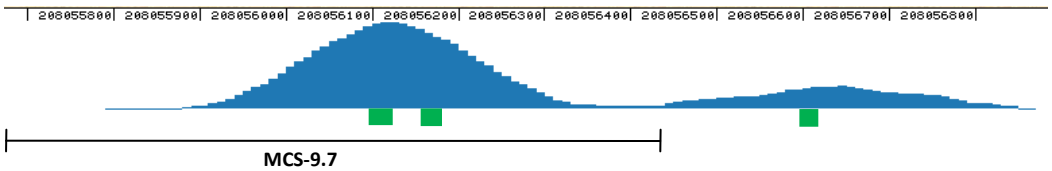

Peak 229

AGTAATACCCCAGGATGTGAACATGTGTGACCATCTGCCTGTCCTGGGGGTGGG
AAGAAGGCAGCATGCTCTATCCTTGACCCTGATTGAGCCCAGGGGCTGAATCTG
GAGCTTTGGGGCCTGGGAACCTCTCTACCTGCGTCAATGTCTGGAGGCCCTGAG
AGTTTCGCTCAGGCTCAGAGCAGGCATCGCAACCTCCCAGTTACTATTCTGTGC
TGTGGCAAGTGCCAGCTTGTCCTCTCTTCCCCACCCAGCCCGGGAAACCGGCAG
CATTTCTAGTTCAGGCCCAGACCCGTCCTGGCAGCCTGGATTCCACTGCCTAGG
CAGGAAGCTCATCTCAGCCCAGTGACCTTTTCTCTCTGTTTTTTGTCACAGAGG
AATTTCCATGCCAGCAGTATGGGGCAATGGGGGTGGGTGGCCAAAGGTTTCCCC
CTTAAGCCACAAGAGCCATGGAGTGGAGGTAAGCTAAGCAAACAGAGGAGGAAG
GATGGGAGGGAAGGATCA

Peak 58

GGAAGATTTAGAGAGTCCATTCCTCAGGCTGCTTCATCCTCAAATTCCAAGGTAA
ATAAAGGTGTTGGGAAGGATGCACTATATGTCCAGCTGCCCAGCCCTGAAGATCC
TCCCCCTAGAGAACTGAGACAGGAGTTTTCTCACATTCCCACATGCAGGAGGGAA
AGAGGCTGGGCCTGGGCAGGTCTAGAGAGTTCTGTTCCCCTGCCCCAGGGGAACA
CGCCTAGGCTTGCTGACCTCTCAGGTAGGAGTCTGTCAGGTTGGAAGCTGGGCCT
CTCATTGTGTGTGTGTGTGTGTGTGTGTGTGAGAGAGAGAGACACGTGTGTGT
GTGTGTGTGTGTGAGAGAGAGAGACACGTGTGTGTGTGTGTGTGTGAGAGAGA
GAGACACGTGTGTGTGTGTGTGTGTGTGTGTGTGTGTGTGTGTGTGTGTGT
ATTGGGGGAGAGAAGCATATAGGATAGGGTGGCCAGAT

p63 motifs
AP-2 motifs
N SNPs

Supplementary Figure 3. **Analysis of binding motifs of p63 and AP-2α in the enhancer element for IRF6.** A zoomed in screenshot of the double peak of p63 binding site upstream of *IRF6* is shown in the upper panel and the corresponding sequences are shown in the lower panel. The MSC-9.7 region is a recently reported enhancer element for *IRF6* identified by multispecies conservation alignment analysis (13). Binding motifs for p63 identified using p53scan are shown in yellow. Motifs for AP-2 α identified with Transcription Element Search System (TESS; http://www.cbil.upenn.edu) shown in blue appear to be degenerate and are located throughout the peak region. The boxed nucleotides are known SNPs and the SNP rs642962 associated with higher risk for cleft lip (13) is indicated with a red box.

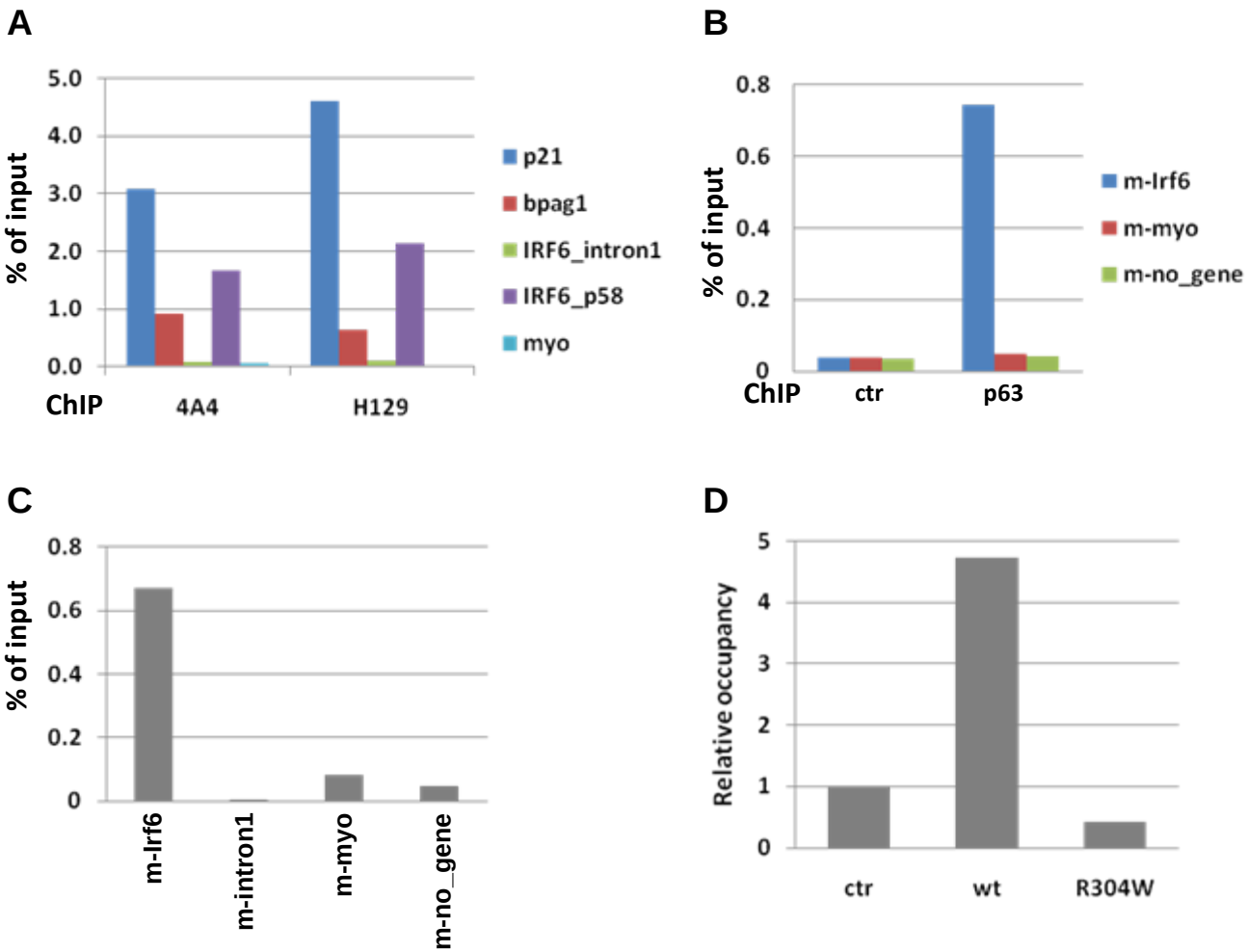

Supplementary Figure 4. ChIP-qPCR analysis of p63 binding sites near the *IRF6* gene in human primary keratinocytes, mouse palatal shelves and in SAOS-2 stable cell lines expressing p63. (A) ChIP-qPCR analysis of p63 binding was performed in human primary keratinocytes using two different p63 antibodies [4A4 (pan-p63) and H129 (α-specific)]. Specific binding of p63 to the reported binding sites upstream of the *IRF6* gene (IRF6-p58), but not to the putative site in the first intron region (IRF6_intron1) was observed. Promoter regions of p21 and BPAG were used as positive controls and that of myoglobin exon 2 (myo) as the negative controls. (B, C) Mouse palatal shelves were dissected from E13.5 embryos and used for ChIP-qPCR analysis using antibody 4A4. IgG was used for control ChIP (ctr in B). In mouse palatal shelves, p63 binds specifically to the upstream enhancer region of Irf6 (homologous to p229 region in human) but not to intron 1 and negative control genes (myo and no gene). (D) ChIP-qPCR analyses performed with antibody 4A4 in SAOS-2-inducible cell lines expressing ΔNp63α wild-type (wt) and mutant R304W proteins show abolition of p63 binding as a result of the R304W mutation.

Supplementary Table 1. Cloning primers for peak 229 region in the p63 binding site

Primers	Sequences
IRF6_cloning_p229_FW	gggg**acaagtttgtacaaaaaagcaggcttcTGTGTGACCATCTGCCTGTC**
IRF6_cloning_p229_RV	gggg**accactttgtacaagaaagctgggtgGCTTAAGGGGGAAACCTTTG**
IRF6_SDM_p229_M1_FW	CTGTGCTGTGGAAAATGCCAGATTATCCTCTCTTCCCC
IRF6_SDM_p229_M1_RV	GGGGAAGAGAGGATAATCTGGCATTTTCCACAGCACAG
IRF6_SDM_p229_M2_FW	GCATTTCTAGTTAAGACCCAGAACCATCCTGGCAGCC
IRF6_SDM_p229_M2_RV	GGCTGCCAGGATGGTTCTGGGTCTTAACTAGAAATGC

Supplementary Table 2. Primers for RT-qPCR analysis

Primers	Sequences
IRF6_exp1_FW	TAGAGAAGCAGCCACCGTTT
IRF6_exp1_RV	GCCACTACTGGAATGACCTGA
IRF6_exp2_FW	TTCTGGTGGACAGATTGAGC
IRF6_exp2_RV	AGGGCCATGATATGGAAGAG
IRF6_exp3_FW	CAAGTGTGTGACATCCCTCAG
IRF6_exp3_RV	CCACATCATTATCCTTCTCATCC
hARP_exp_FW	CACCATTGAAATCCTGAGTGATGT
hARP_exp_RV	TGACAAGCCCAAAGGAGAAG
mIrf6 F	AGGGCTCTGTCATTAATCGAG
mIrf6 R	TGATTCGGGGCTGCAGTTTC

Supplementary Table 3. Primers for ChIP analysis

Primers	Sequences
IRF6_ChIP_p229_FW	ACCGGCAGCATTTCTAGTTC
IRF6_ChIP_p229_RV	ACTGGGCTGAGATGAGCTTC
IRF6_ ChIP_p58_FW	TTTCTCACATTCCCACATGC
IRF6_ ChIP_p58_RV	CCAACCTGACAGACTCCTACC
p21_ChIP_FW	GTGGCTCTGATTGGCTTTCTG
p21_ChIP_RV	CTGAAAACAGGCAGCCCAAG
BPAG_ChIP_FW	TCCTGGACATCTGTGAGGCA
BPAG_ChIP_RV	CCAATTGCAACCACCTAAAAAAC
myo ex2_FW	AAGTTTGACAAGTTCAAGCACCTG
myo ex2_RV	TGGCACCATGCTTCTTTAAGTC
chr11_nogene_FW	TTGCATATAAAGGAAACTGAAATGCT
chr11_nogene_RV	TTACTGCCATGGGTCCGTATC